Anal. Bioanal. Electrochem., Vol. 13, No. 2, 2021, 239-263

Analytical &
Bioanalytical
Electrochemistry

Full Paper

Electrochemical Corrosion Behavior of API 5L X52 Pipeline Steel in Soil Environment

Sonia Mameri,[1,2,*] Dalila Boughrara,[1] Jean-Paul Chopart,[2] and Abdelaziz Kadri[1]

[1]*Laboratoire de Physique et Chimie des Matériaux, Université Mouloud Mammeri de Tizi-Ouzou, BP 17 RP, Tizi-Ouzou 15000, Algérie*

[2]*Ecole d'Ingénieurs en Sciences Industrielles et Numérique, Université de Reims Champagne Ardenne, 9, bd de la PAIX. 51 097 REIMS cedex, France*

*Corresponding Author, Tel.: 00766386990

E-Mail: sonia.mameri@etudiant.univ-reims.fr

Received: 8 February 2021 / Received in revised form: 5 August 2021 / Accepted: 30 August 2021 / Published online: 30 September 2021

Abstract- In this work, the corrosion rate of X52 pipeline steel used in Algerian soil was calculated and compared to that of a simulated soil solution (NS4). The effect of soil related parameters such as pH, temperature and immersion time on the corrosion of steel in NS4 solution is studied using different methods such as open circuit potential, potentiodynamic polarization, electrochemical impedance spectroscopy and energy dispersive spectrometry (EDX) coupled with scanning electron microscopy. The results are well correlated and showed that the corrosion rate increases when the medium is acidic or alkaline and when the temperature increases. The load transfer resistance increases with immersion time up to 3 days and then decreases with the presence of a film of corrosion products on the steel surface which becomes porous. It was also found that the corrosion rate of X52 steel immersed in the aqueous soil extract collected in southern Algeria is the lowest.

Keywords- API 5L X52 Steel; NS4 Solution; Aqueous soil extract; Polarization; EIS

1. INTRODUCTION

In the world, crude oil, refined petroleum and gas transport by pipelines partially or completely buried in the ground are the most efficient means and currently represents 66.3%

of the pipelines operated worldwide [1,2] with enormous advantages. The first pipeline was built in 1869 by Benson to avoid the monopoly of oil transport by rail. Pipelines allowed the exchange of products between refineries, oil depots, oil tankers and ports. Its length can vary from a few kilometers to hundreds or even thousands of kilometers. Pipelines are often interconnected to form a network [3]. Depending on the nature of the fluid transported, professionals distinguish between oil and gas pipelines in the case of petroleum and gas.

A pipeline is characterized by its line consisting of steel tubes with a common diameter of between 15 cm and 1 meter and a thickness of 4 to 13 mm. The depth of burial in the ground varies from 0.6 to 1 m depending on its length of service and its locations. Among the most decisive advantages are the mass transport of about 60×10^6 L/days, uninterrupted operation (24 hours a day, 365 days a year), transport with a high degree of safety, energy efficiency due to the fact that it is not encumbered by surface infrastructure, cheaper mode of transport over long distances, and for high volumes. In Algeria, the production and transport of hydrocarbons, crude oil and gas use more than 3.7×10^6 km of pipelines. Carbon steels are the most widely used steels in pipeline construction [4], due to their low cost, control of the techniques of their development and their production. These steels are usually in grades such as X60, X65, X80, X52, X70, etc. [5,6].

Indeed, the failure of these steel structures and the limitation of their lifespan by the phenomenon of corrosion is the main concern of researchers. Oil fields are the greatest victims of corrosion phenomena, more particularly, the pipeline networks. This devastating phenomenon causes serious environmental and economic problems [7,8]. In Algeria, a study was carried out by Boukhallat [9], based on real data specific to the Hassi Messaoud field. This study gave the evolution of the number of leaks as a function of the years, and which would be close to 1800 in 2005. The majority of leaks on pipelines are primarily the result of internal corrosion, accentuated by external corrosion. These leaks can cause serious accidents, such as the fire that occurred on 21 September 2004 on the GZ 2 gas pipeline between Hassi-R'mel and Arzew in the locality of El-Ghomri [10], 53% of failures are due to internal corrosion and 12% to external corrosion [11]. However, up to now, with regard to the study of the behavior of steel against corrosion in the specific soil of southern Algeria, there is little research.

The corrosion of steel in soil depends on the aggressiveness of the soil in which the pipe is buried and is strongly conditioned by the environment in which they are located. Due to the complexity of the soil and its porosity, the study of the corrosion mechanism of structures buried in the ground is quite difficult, and differs from place to another, which is why more and more attention must be paid to this field of study and a better understanding of the soil is necessary to provide adequate protection for buried pipelines [12]. Therefore, it is necessary to study their corrosion mechanisms in a real soil environment or in the aqueous extract of the soil of a region of passage of the buried pipes.

In the context of corrosion, buried pipelines in the ground are subject to acidic, neutral and basic soil environments and to different climate changes over time, such as soils rich in organic matter and mineral soils when moistened by rainwater they become acid [13] which cause their degradation over time resulting in very significant economic and human losses.

Factors that significantly influence steel corrosion in the soil include: moisture content, resistivity, pH, temperature variation, oxygen concentration, oxidation-reduction potential, soil texture, bicarbonate, chloride and sulphate ions content and microorganisms [13-15]. However, several studies have been carried out on the simulation of corrosion in the soil environment with the influence of many parameters. For example, the corrosion of buried steel is affected by the size of the soil grains. He and al [16-19] studied the effect of soil texture on the electrochemical corrosion behaviour of X70 pipeline steel in NaCl-based corrosive sandy soil environment. The results indicated that the corrosion rate of the X70 steel increases with the decrease in soil particle size. Benmoussa and al [13] have highlighted the effect of resistivity, pH, temperature, and soil moisture content on the corrosion behaviour of X60 pipeline steel in a simulated NS4 soil solution. They deduced that the corrosion current density and activation energy increases with temperature and with moisture content when soil resistivity decreases. Ikpi and al [20] reported the effect of pH and temperature on corrosion of API 5L X52 steel in simulated soil solutions and deduced that steel corrosion increases as the temperature increases and also with increasing acid conditions. The influence of temperature on corrosion of pipeline steels in deep-sea environment was studied by Wang and et al. [21] which revealed that the film density of the corrosion layer decreases with increasing temperature as a result of increased corrosion. Other studies [22] found that corrosion rate of API X80 steel was increased with temperature and pitting corrosion was observed at low temperatures. Another attempt using impedance diagrams and micro-structural analysis has been used by Corrales-Luna [23] to evaluate the corrosion of API 5L X52 steel exposed to an aqueous saline medium (ASM), showed the formation of porous corrosion films in the presence and the absence of oxygen at different exposure times and temperatures. Other studies were conducted by Wu and al. [24] on the influence of pH on the corrosion of Q235 steel in simulated soil solutions from Yingtan where they reported that the corrosion rate decreased with the increase in pH from 3 to 7.

In this present study, we purpose to evaluate the electrochemical corrosion behaviour of API 5L X52 pipeline carbon steel in simulated soil solution NS4 by varying three parameters, immersion time, pH and temperature using potentiodynamic polarization and electrochemical impedance spectroscopy (EIS). Furthermore, this paper propose a characterization of the corrosion process of X52 steel in a specific soil of a pipeline location in southern Algeria in comparison with a similar soil solution, and allows to give a first idea to the industrialists. The kinetic parameters and the corrosion mechanism under these conditions were analyzed. These results will inform about the lifetime of the pipelines and allow reducing service disruptions and to predict inspection and control programs.

2. EXPERIMENTAL SECTION

2.1. Microstructure of the steel

The API 5L X52 carbon steel used in this work has been recovered from the pipelines used by Sonatrach to transport gas and oil in southern of Algeria. Table 1 presents the nominal chemical composition of the test material.

Table 1. Chemical composition of API X52 carbon steel (wt. %)

C	Cr	Ni	Mn	Si	Cu	Co	S	P	Al	Mo	Nb	Fe
0.1805	0.018	<0.001	0.908	0.276	0.016	0.010	0.010	0.009	<0.001	0.003	<0.001	Bal.

In order to observe the microstructure of the sample, etching with 2% Nital solution (2% nitric acid + 98% ethanol) was used; the analysis was performed using the scanning electron microstructure (SEM) observation, as shown in Fig. 1. The structure consists mainly of polygonal ferrite (dark grey areas) and granular pearlite (light areas), which is characteristic of the microstructure of low strength pipeline steels. This is in agreement with similar microstructures obtained by others [25-27].

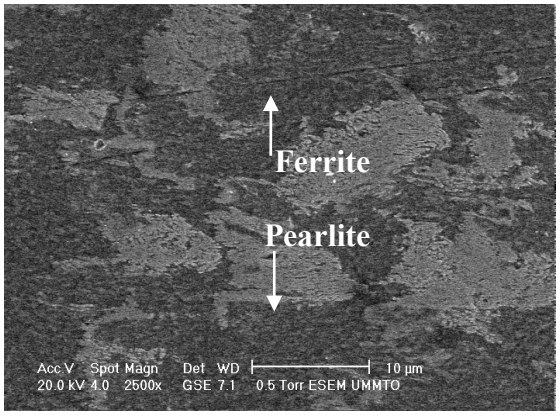

Fig. 1. Microstructure of X52 pipeline steel chemically etched with a 2% nital solution

After each electrochemical test, scanning electron microstructure coupled to energy-dispersive X-ray spectroscopy (SEM-EDS) analysis was performed for the steel samples to characterize the morphology of each sample and to identify the corrosion type generated at the steel surface.

2.2. Steel preparation

The steel samples were cut using a cutting machine, coated with a polymerizable resin (Bakelite) after applying a layer of varnish, to ovoid crevices in samples, leaving an exposed

surface area of 0.48 cm^2. Before each test, the surface was polished with silicon carbide abrasive papers of different diameters ranging from 120 µm to 1000 µm under water using a USCIL-ESC 250 GT lapping/polishing machine. A finishing polishing was carried out with a 1 µm alumina suspension to obtain a mirror appearance. The steel sample was then rinsed with distilled water, then subjected to an ultrasonic cleaning bath for 2 minutes in acetone and finally dried with cold air.

2.3. Solution test

The synthetic test solution (NS4) was prepared from analytical grade reagents and distilled water. It has a pH 8.3 and a chemical composition given in Table 2.

Table 2. Chemical composition of the NS4 solution [28]

Component	$CaCl_2$	$MgSO_4$	KCl	$NaHCO_3$
Concentration (g/L)	0.181	0.131	0.122	0.483

The aqueous extract of the soil is prepared as follows. Sandy soil sample was taken from 1 m of depth from the ground level in southern Algeria. 200 g of dry soil and 1 liter of distilled water were poured into a volumetric flask and agitated for 3 hours, then left to rest for one night. After settling the soil, the liquid phase (aqueous extract) was obtained by filtration. The pH of the obtained aqueous extract is 7.5. The value is an indicator of excess calcium carbonate [29].

Soil pH is probably the single most informative measurement that can be made to determine soil characteristics.

In order to study the influence of pH solution, the pH of the NS4 solution is varied and adjusted by adding H_2SO_4 0.2 N or NaOH 1 N. The pH adjustment is also realized in order to obtain the two electrolytes (NS4 and extract soil solution) at pH 7.5.

The conductivity of the NS4 solution (900 µS/cm) was higher than the conductivity of the aqueous soil extract (381 µS/cm).

2.4. Electrochemical measurements

To determine the corrosion resistance of X52 pipeline steel, potentiodynamic polarization and electrochemical impedance spectroscopy (EIS) were performed in the aqueous soil extract and in simulated NS4 soil solution using a Potentiostat-Galvanostat AUTOLAB PGSTAT-30.A three-electrode cell is adopted using pipeline steel X52 as the working electrode, the Ag/AgCl/KCl as the reference electrode and platinum (Pt) as the auxiliary electrode. For the polarization curves, the electrode potential was swept from -1 V *vs.* Ag/AgCl to open circuit potential (OCP), and then to +300 mV above OCP, starting from the cathodic to the anodic

domain at a scan rate of 1 mV/s. For Tafel analysis, the polarization range was about 300 mV or 400 mV below and above the corrosion potential (E_{corr}).

EIS spectra were obtained at OCP and after the OCP of the steel reached a steady state by applying AC signal amplitude of 10 mV in the frequency range 10 kHz to 10 mHz. The impedance data were fitted with the equivalent electrical circuit using the EquivCrt program in FRA software.

These experiments were performed for different immersion times (0h up to 15days), temperatures (25, 35, 45 and 55°C) and pH values between 4 and 10. All tests were repeated three times to ensure reproducibility.

3. RESULTS AND DISCUSSION

3.1. Influence of immersion time

In order to follow the effect of immersion time on the corrosion of the API X-52 pipeline steel, we carried out OCP, impedance and polarization measurements after 0, 1, 6 and 24h and for long time, 3, 5 and 15 days of immersion in NS4 solution of pH 8.3 at 25°C.

3.1.1. OCP measurement

Fig. 2 shows the evolution of the OCP of the X52 pipeline steel sample immersed in aerated NS4 solution (pH 8.3) as a function of immersion time at ambient temperature.

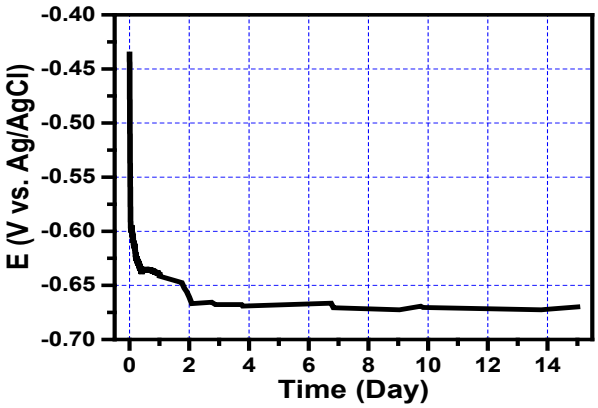

Fig. 2. Evolution of OCP versus time for the X52 steel in NS4 solution of pH 8.3 at room temperature

The OCP of the sample shifts towards negative values as a result of a spontaneous dissolution and corrosion of the metal surface. It can be observed that the OCP decreases rapidly in the first time of immersion and after 5 hours of immersion it stabilizes around a value of the order of -0.67 V *vs.* Ag/AgCl. This result is a characteristic value of carbon steel compared to the literature.

3.1.2. Electrochemical impedance spectroscopy

Fig. 3 shows the Nyquist diagrams and Bode plots of steel sample obtained after different immersion times in NS4 solution. The impedance diagrams consist of one depressed incomplete capacitive semicircle which is due to the charge transfer resistance and the double layer capacitance.

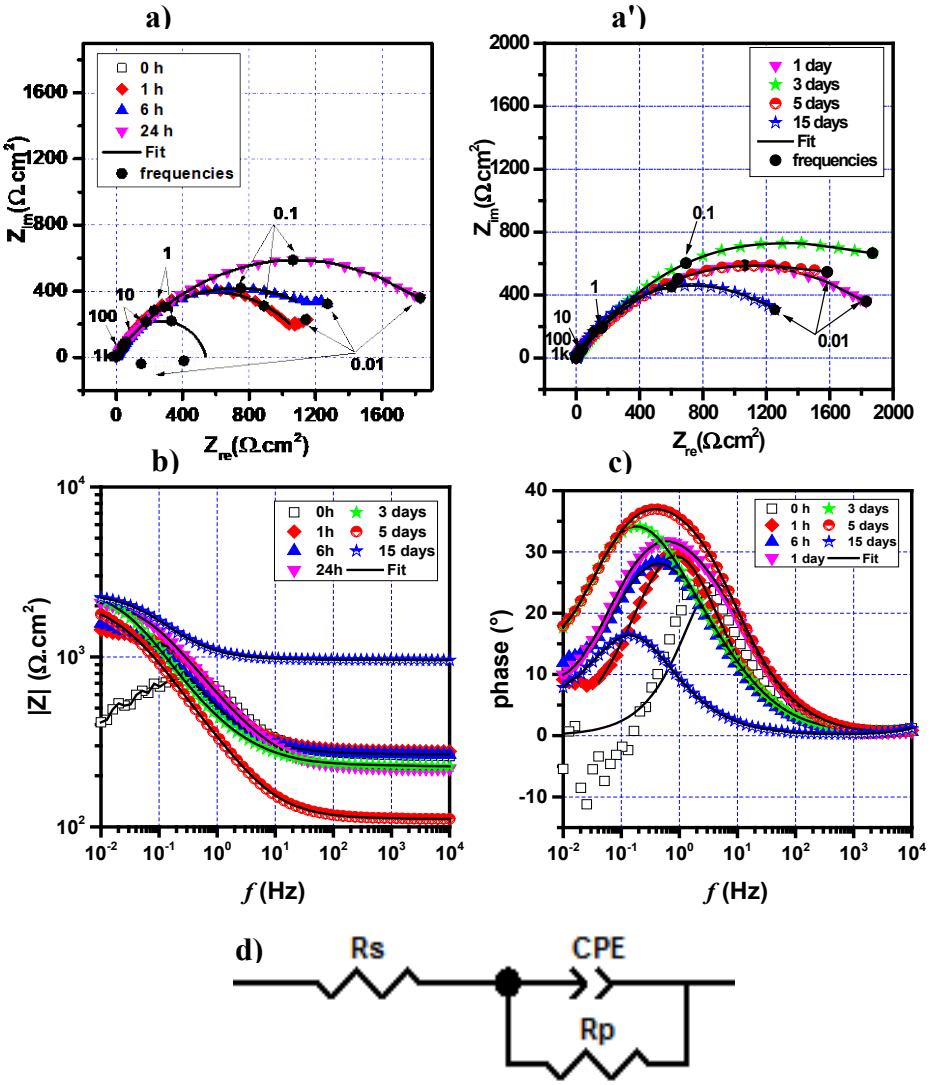

Fig. 3. a) Nyquist diagrams, b) and c) Bode plots of X52 steel at different immersion times in NS4 solution of pH 8.3 at room temperature; d) Electrical equivalent circuit used to fit the EIS experimental data

At low frequencies, the onset of a second capacitive loop is observed for 1 and 6 h and then disappears over time, which may be due to a diffusion effect, attributed to the transport of oxygen through holes and pores. The Nyquist plots feature of one semicircle, combining with one maximum phase angle in Bode plots (Fig. 3c), indicates the impedance behavior with one time constant.

The capacitive loop is fitted using the electrical equivalent circuit (EEC) depicted in Fig. 3d. The EEC parameters correspond to a solution resistance, R_s, connected with the parallel connection of a charge transfer resistance, R_{ct}, and double layer capacitance replaced with a constant phase elements, *CPE*, with its parameters (n and Q). The CPE was explained by the heterogeneity of the electrode/solution interface. For quantitative comparisons of the effect of time on the steel corrosion, the EIS parameters of the equivalent circuit presented in Fig. 3d, are listed in Table 3.

Generally, the size of the semicircle is inversely proportional to corrosion rate of the steel. The size of the semicircle increases steadily up to 3 days and then reduces with time. The EIS parameters recorded in Table 3 also indicate an increase of R_{ct} value with immersion time from 0 to 3 days, which is representative of an improvement of corrosion resistance and inversely a decrease of the corrosion rate for the X52 steel with time. This result suggests the formation of a protective film usually formed of corrosion products on the steel surface whose protection becomes low with immersion time. After 3 days, the polarization resistance starts to decrease which means that the film loses gradually its aptitude to well protect the steel surface by becoming porous.

The lowering of n values with time indicates that the electrode surface becomes more heterogeneous and suggests a contribution of the mass transport process throughout the pores of the corrosion products layer or adsorption process according to Ikpi and al [20]. After 3 days, slightly increase of n value is associated with an activation of the surface due to dissolution and desorption of some corrosion products.

Table 3. Electrical parameters obtained by fit EIS data

Time	R_s ($\Omega.cm^2$)	Q ($\Omega^{-1}.cm^{-2}.s^n$)	n	R_{ct} ($\Omega.cm^2$)
0 h	265	2.40×10^{-4}	0.87	530
1 h	280	5.67×10^{-4}	0.75	1177
6 h	267	8.44×10^{-4}	0.66	1461
1 day	155	14.00×10^{-4}	0.64	1670
3 days	82	11.33×10^{-4}	0.60	2600
5 days	111	10.66×10^{-4}	0.65	2450
15 days	956	15.35×10^{-4}	0.67	1760

Bode plots (Fig. 3b) shows one time constant related to the electrical properties of the steel/soil solution interface. However, this inflection points is displaced toward lower values when exposure time increases.

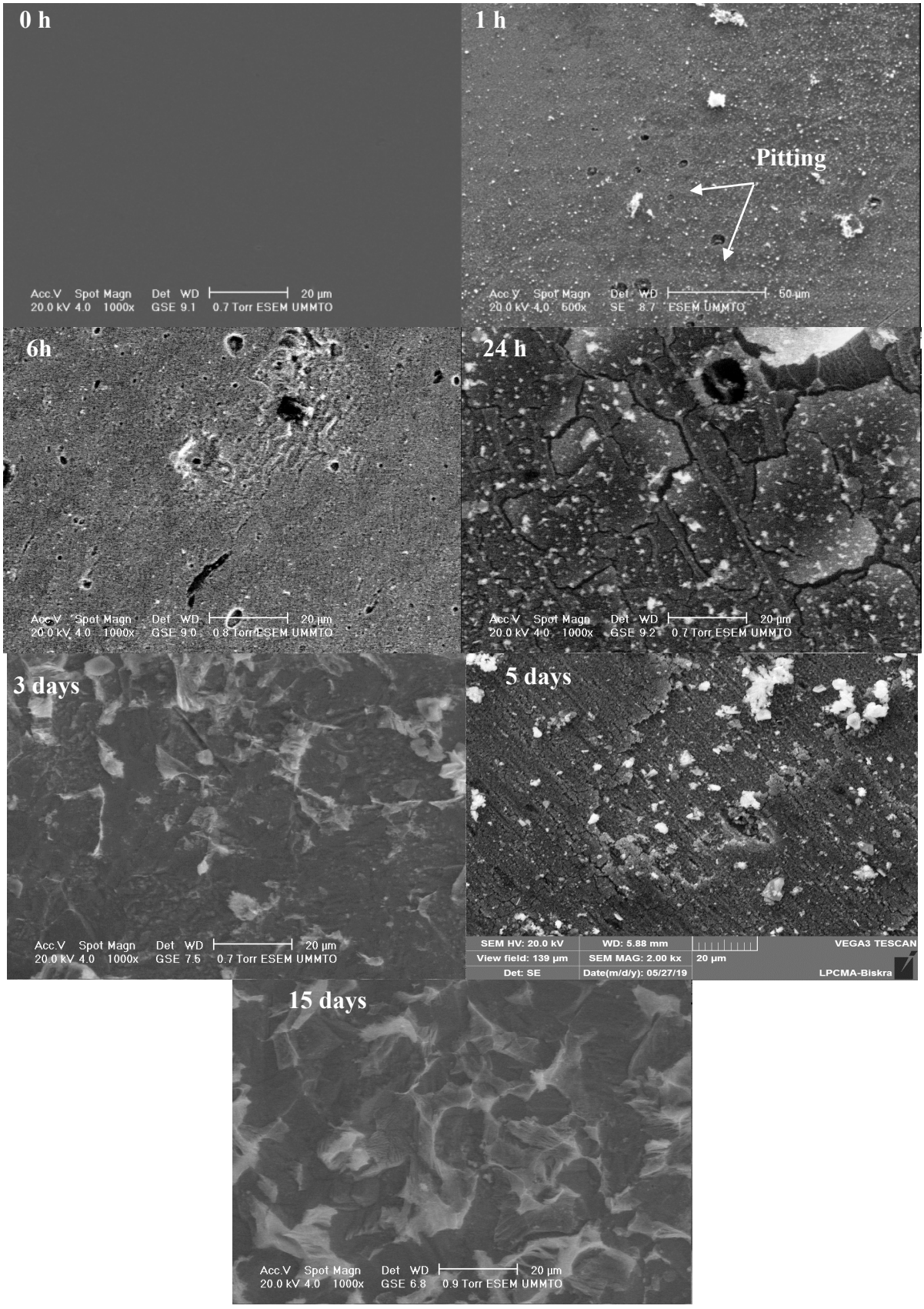

Fig. 4. SEM images of steel surface obtained in NS4 solution after different immersion times

3.1.3 Morphology of the surface

The SEM images of steel surface obtained in NS4 solution after different immersion times are presented in Fig. 4. As can be seen, in low immersion time (1 h), the formation of pits is in the induction stage and white products forms that may be precipitates of the solution's compounds and/or the corrosion products. Besides, the surface is attacked with increasing immersion time, the products grow and compact layer is obtained which could be carbonated iron oxides with different compositions, aragonite, calcite as found by a previous study [30]. According to observations for very high immersion time (image 5 days), internal stress increases the pores and cracks in the corrosion products layer. The pores facilitate the diffusion of reaction products across the layer and the access of oxidants to the surface of the material, which reduces corrosion resistance.

3.1.4. Potentiodynamic polarization curves

Fig. 5 shows the potentiodynamic polarization curves of X52 steel after different immersion times in the simulated soil solution (NS4). The evolution of the corrosion rate and the polarization resistance are presented in Fig. 6. The values corrosion parameters, cathodic (b_c) and anodic (b_a) Tafel slopes, corrosion potential (E_{corr}), corrosion current density (i_{corr}), polarization resistance (R_p) and corrosion rate (CR), are reported in Table 4. It can be noted that the results were determined using the Tafel extrapolation method.

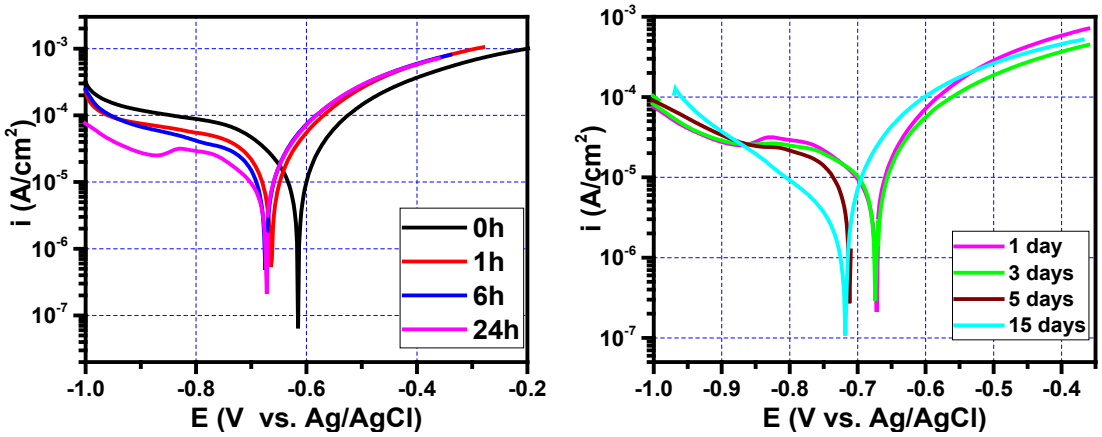

Fig. 5. Potentiodynamic polarization curves of carbon steel X52 after differentimmersion timesin NS4 solution of pH 8.3 at room temperature

The Stern-Geary equation is utilized to calculate the R_p [31]:

$$R_p = \frac{1}{i_{corr}} \times \left(\frac{b_c \times b_a}{2.3(b_c + b_a)}\right) \quad (1)$$

$$R_p = \frac{\Delta E}{\Delta I} = \frac{B}{icorr} \quad (2)$$

where $$B = \frac{ba \times bc}{2.3\ (ba + bc)} \quad (3)$$

The Stern-Geary constant, B, was calculated using the cathodic and anodic Tafel slope values based on the Tafel analysis of the polarization curve.

The corrosion rate, CR, is calculated using the following relation [32-35]:

$$CR = \frac{i_{corr} \times k \times EW}{d} \quad (4)$$

where, i_{corr} is the corrosion current density in A/cm^2, k is a constant that defines the units of corrosion rate (k = 3272 mm/ (A.cm.year)), EW the equivalent weight for the iron alloy in grams/equivalent (EW = 27.93 grams/equivalent) and d is the low carbon steel density in g/cm^3 (d = 7.86). Hence, *CR (mm/year)* = 11627×i_{corr}.

In the solution test, the predominant reactions that can occur during the cathodic and anodic polarization are the reduction of oxygen and iron dissolution, respectively. All the anodic curves show a similar behaviour without passivation phenomenon. Initially, the current densities increase with time then decrease for long time. In the first time, the surface electrode is active because the corrosion products have not yet formed. Over time, the decrease of current densities can be related to the reduction of the active surface in contact with the electrolyte as a consequence of its covering by the corrosion products. The bounce in the current suggests that product layer does not have a corrosion protection effect due to the increase of its porosity and cracking (Fig. 4).

However, the cathodic polarization curves present a current density plateau characteristic for the diffusion-limited oxygen reduction which gradually flattens out with immersion time and tends to disappear if the immersion time is too long. In addition, the decrease of cathodic slopes may suggest the formation of corrosion products layer on the steel surface that reduces the active surface and becomes as a barrier layer that prevents the access of oxygen.

This was further confirmed by the corrosion parameters that are listed in Table 4.The increasing of the immersion time shifts the E_{corr} slightly towards more negatives values. As expected, i_{corr} and CR decreases as time elapses, inversely proportional to R_p (Fig. 6); it could result from the deposition of corrosion products with time which block the surface (Fig. 4 SEM). However, the surface is subjected to pitting corrosion and the surface is not protected.

Table 4. Values of electrokinetic parameters determined from polarization curves

Time	E_{corr} (mV *vs.* Ag/AgCl)	i_{corr} (μA/cm^2)	$-b_c$ (mV/dec)	b_a (mV/dec)	R_p (Ω.cm^2)	CR×10^{-4} (mm/y)
0 h	-616	32.6	359	179	1593	3790
1 h	-663	26.9	383	186	2039	3128
6 h	-675	20.0	480	140	2356	2330
1 day	-673	8.3	191	87	3180	965
3 days	-674	8.1	185	90	3250	942
5 days	-713	7.5	141	-----	----	872
15 days	-720	3.0	150	60	6211	349

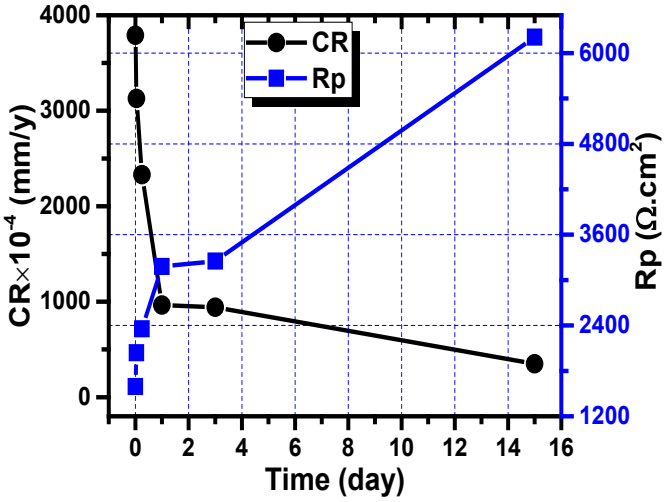

Fig. 6. Evolution of the corrosion rate and the polarization resistance of carbon steel X52 versus immersion times in NS4 solution

3.2. Influence of pH

In order to study the effect of the solution pH on the corrosion of the API X-52 pipeline steel, we report OCP, impedance and polarization measurements at pH 4, 5, 7, 8 and 10 after 24h immersion in NS4 solution at room temperature.

3.2.1. Evolution of the open circuit potential

Fig. 7 shows the evolution of the open circuit potential of X52 steel as a function of the pH solution.

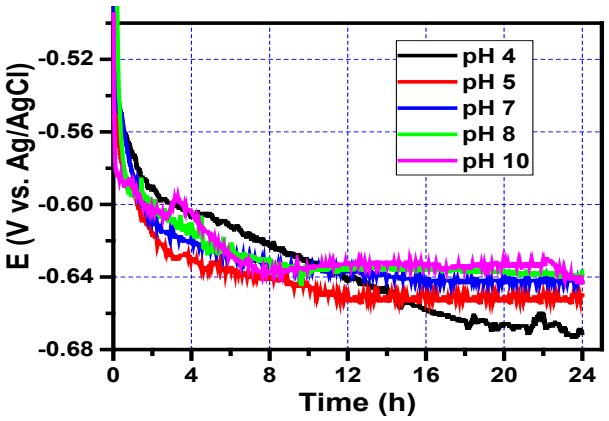

Fig. 7. Evolution of corrosion potential of X52 steel in a simulated soil solution as a function of pH during 24 hours of immersion at room temperature

It has been noted that the open circuit potential of X52 steel decreases rapidly in the first few hours, then the decrease slows down over time. This appearance indicates a spontaneous

dissolution of the sample.The fluctuations observed on the curves, associated with the potential instability, indicate non-uniform corrosion (pitting corrosion).

At acidic pH (4 and 5), the potential shifts to more negative values (-0.67 V/Ag-AgCl and -0.65 V/ Ag-AgCl, respectively) compared to the potential of the neutral solution (pH 7). For alkaline pH, the OCP stabilizes at higher values which increases with pH (-0.64 and -0.635 V/Ag-AgCl for pH 8 and 10, respectively). At pH 10 we notice that the corrosion potential of the steel is stable until 22 hours of immersion and then it decreases in the last moments, this can be attributed to the detachment of products formed on the surface hence an activation of the corrosion.

3.2.2. Electrochemical impedance spectroscopy

The EIS results for API 5L X52 carbon steel in NS4 simulated soil solution at different pH levels after 24 hours of immersion time are shown in Fig. 8. The values of the electric parameters obtained after fitting with EEC are presented in Table 5.

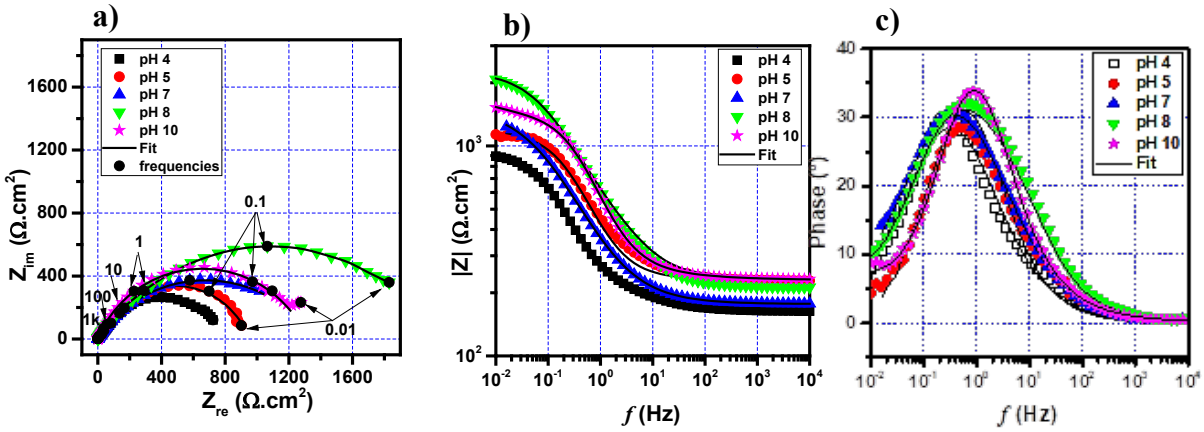

Fig. 8. a) Nyquist diagrams, b) and c) Bode plots of X52 steel in simulated soil solution (NS4) at different pH at room temperature

All impedance diagrams obtained at different pH levels (4, 5 and 8), are identical to those in Fig. 3; one incomplete depressed semi-circle. It is seen that, the diameter size increases with the pH of the NS4 solution up to pH 8, where the highest R_{ct} value is obtained, indicating the lowest corrosion rate under these conditions.

At pH 10, the formation of precipitates is probably high but we notice that the semi-circle has decreased compared to that of pH 8, which indicates an increase in corrosion rate, in this case we can say that the corrosion products and precipitates formed during the immersion period have been detached from the surface at the time of the EIS measurement. At low frequencies, the appearance of a beginning of diffusion process is probably due to the transport of the corrosion products through the porous corrosion product layer. The n values are less than 1 (between 0.62 and 0.79), which means that the surface is really heterogeneous.

Table 5. Electrical parameters obtained by fit EIS data

pH	R_s ($\Omega.cm^2$)	Q ($\Omega^{-1}.cm^{-2}.s^n$)	n	R_{ct} ($\Omega.cm^2$)
4	166.2	0.18×10^{-2}	0.69	851
5	231.1	0.82×10^{-3}	0.79	950
7	176.7	0.12×10^{-2}	0.64	1355
8	154.5	0.14×10^{-2}	0.64	1670
10	234.7	0.52×10^{-3}	0.76	1314

3.2.3. Potentiodynamic polarization curves

Fig. 9 illustrates the potentiodynamic polarization curves of steel X52 in the NS4 solution obtained after 24 hours of immersion at room temperature by varying the pH range from 4 to 10. Table 6 presents the values of the polarization parameters as a function of pH.

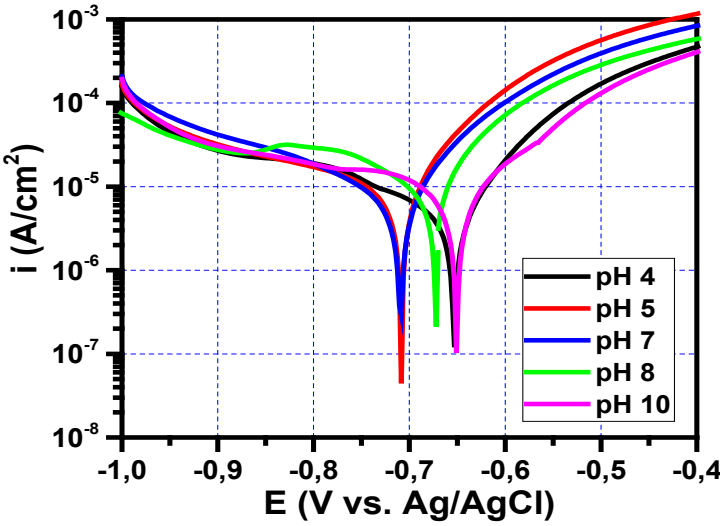

Fig. 9. Potentiodynamic polarization curves of carbon steel X52 at different pH values in the simulated soil solution (NS4)

In the studied pH range, all polarization curves have the same shape indicating a same corrosion processes, and show a considerable increase in corrosion activity as a function of pH in acid environments (pH 4 and 5) and in alkaline one (pH 8 and 10).

The cathodic limiting current density increases with pH. The anodic current density decreases as the pH decreases, in contrast the cathodic current density increases as the pH decreases, while i_{corr} (inversely to R_p) increases with acidity and alkalinity of soil environment (Fig. 10), and this is in agreement with previous findings.

Table 6. Values of electrokinetic parameters determined from polarization curves

pH	E_{corr} (mV/Ag/AgCl)	i_{corr} (µA/cm^2)	$-b_c$ (mV/dec)	b_a (mV/dec)	R_p (Ω.cm^2)	CR×10^{-4} (mm/y)
4	-652	11.0	660	73	2598	1278
5	-708	10.0	388	90	3176	1163
7	-708	6.0	182	79	3991	698
8	-673	8.3	191	89	3180	965
10	-650	14.5	490	100	2490	1686

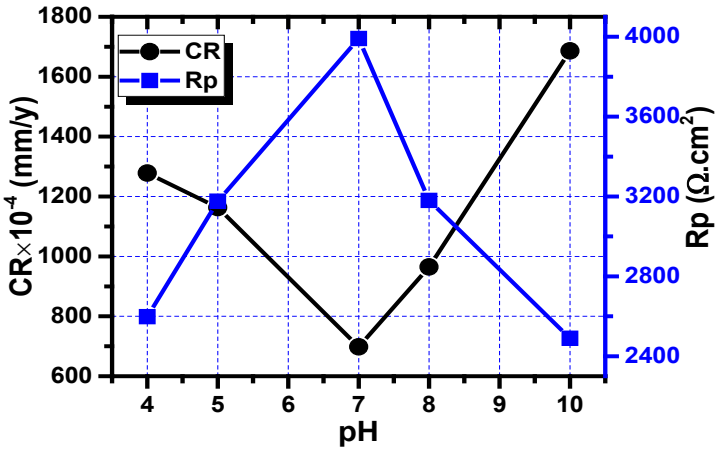

Fig. 10. Evolution of the corrosion rate and polarization resistance of carbon steel X52 versus pH values in the NS4 solution

It is clear that the trends of both curves (corrosion rate and polarization resistance) as a function of pH are assumed. In an acidic and alkaline environment, the corrosion rate of steel is significant, which leads us to conclude that soil acidity is a very important parameter and has a significant influence on buried pipelines.

3.3. Influence of temperature

The resistance ability of the API X52 steel is also studied at different temperatures of 25, 35, 45 and 55°C in the NS4 solution of pH 8.3 during 6 hours of immersion.

3.3.1. Evolution of the open circuit potential

Fig. 11 shows the OCP evolution of X52 steel as a function of temperature. The OCP value shifts to very negative values when the temperature increased from 25 to 55°C and the values gradually decreased from -0.63 to -0.67 V *vs.* Ag/AgCl, respectively. This observation indicates an increase of the dissolution and the corrosion of the X52 steel with temperature, before reaching a quasi-stationary state.

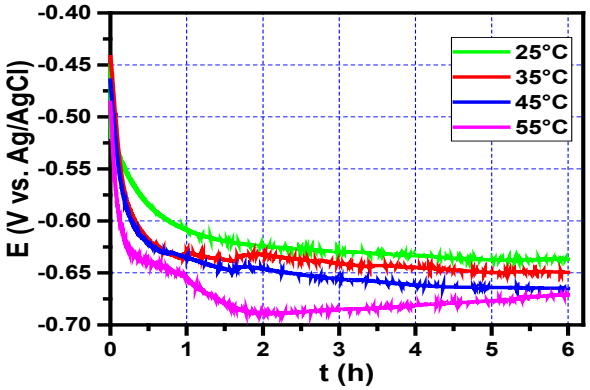

Fig. 11. Evolution of corrosion potential of X52 steel in a simulated soil solution as a function of temperature

3.3.2. Electrochemical impedance spectroscopy

Fig. 12 shows the Nyquist plots of steel obtained after 6 h immersion in the NS4 solution of pH = 8.3, at various operating temperatures. The EIS data are better adapted to the electrical equivalent circuit (EEC) shown in Fig. 3b and the fitted values are presented in Table 7.

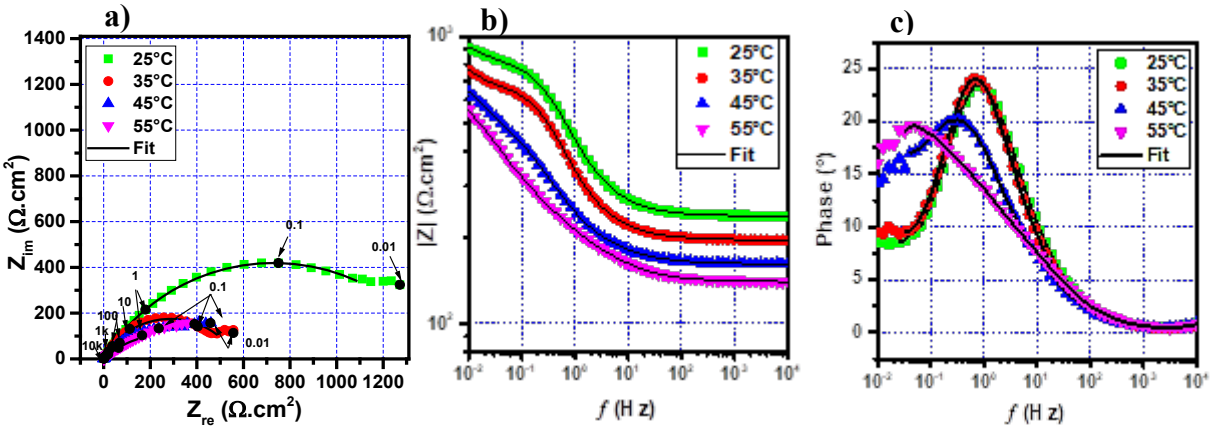

Fig. 12. a) Nyquist diagrams, b) and c) Bode plots of X52 steel after 6 h in NS4 solution of pH = 8.3 at different temperatures

It was noted that the module values of impedances (Fig. 12b) decreased with rising temperature. It is also important to note a clear evolution in the general shape of the plots when the temperature increases. At low temperature the curve has a unique and defined semi-circular shape but at high temperature the curve showed a decrease in the semicircular shape.

The peak of the phase angle diagram (Fig. 12c) flattens out and shifts towards low frequencies, indicating that the layer of corrosion products produced at higher temperatures is thinner than that formed at lower temperatures. It is clear from Table 7 that the resistance (R_s and R_{ct}) values decrease gradually as the temperature is increased which can be due to the ion

activity increase in the solution with an increase of corrosion rate. The increase in temperature accelerates the corrosion phenomenon of steel via increasing the values of i_{corr} and CR. This result is in good agreement with the study of Okonkwo and al [24].

Decreasing values of *n* indicates increasing diffusion contribution and heterogeneity of the electrode surface with temperature as observed on the SEM micrographs shown below (Fig. 16).

Table 7. Electrical parameters obtained by fit EIS data

T (°C)	R_s (Ω.cm^2)	Q (Ω^{-1}.cm^{-2}.s^n)	n	R_{ct} (Ω.cm^2)
25	266.8	0.84×10^{-3}	0.66	1461
35	194.8	0.13×10^{-2}	0.70	573
45	160.4	0.29×10^{-1}	0.59	550
55	137.7	0.44×10^{-2}	0.49	537

3.3.3. Potentiodynamic polarization curves

Fig. 13 shows the polarization curves of X52 steel for different temperatures (25°C to 55°C) in the simulated soil solution (NS4). The parameters values corresponding to the polarization curve are summarized in Table 8.

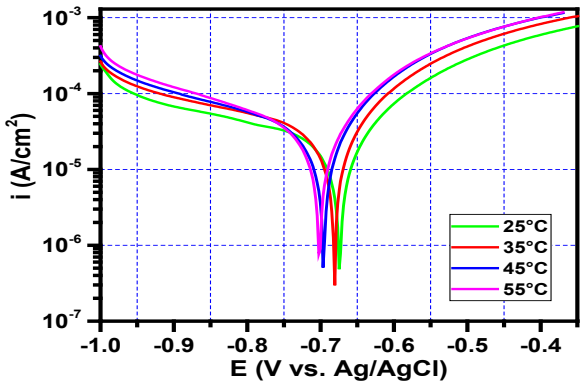

Fig. 13. Potentiodynamic polarization curves of carbon steel X52 after 6 h in NS4 solution of pH = 8.3 at different temperatures

In the studied temperature range, the anodic polarization curves present active corrosion characteristics which increase with increasing temperature and without passivation phenomenon. The increasing temperature shifts the polarization curves to more cathodic potentials in line with the OCP results, which indicates that corrosion process is controlled by the oxygen cathodic reduction. An increase in temperature of 10 °C leads to a linear increase in corrosion current densities and thus the corrosion rate, inversely to the polarization resistance (Table 8 and Fig. 14). This evolution is clearly distinguished by plotting the two parameters as

a function of temperature. This result correlates well with those of the previous techniques and confirms that temperature variation in the soil surrounding the pipeline leads to significant degradation of the pipeline.

Table 8. Values of electrokinetic parameters determined from polarization curves

T (°C)	E_{corr} (mV/Ag/AgCl)	i_{corr} (μA/cm^2)	$-b_c$ (mV/dec)	b_a (mV/dec)	R_p (Ω.cm^2)	CR×10^{-4} (mm/y)
25	-675	20	480	140	2356	2330
35	-680	23	460	145	2085	2670
45	-695	28	380	130	1504	3260
55	-705	30	310	130	1327	3490

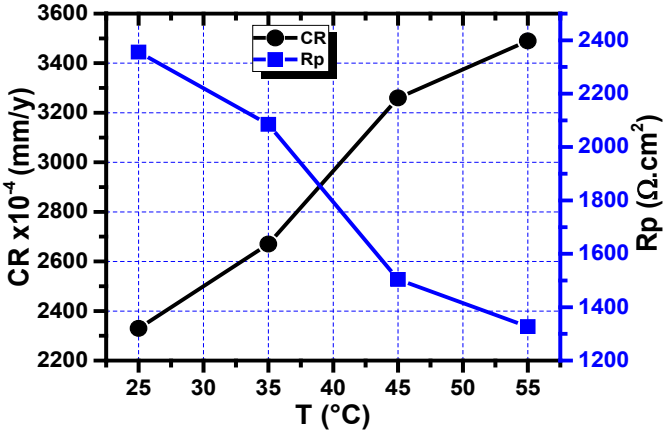

Fig. 14. Evolution of the corrosion rate and polarization resistance of carbon steel X52 after 6 h in NS4 solution of pH = 8.3 as a function of temperature

The Arrhenius formula [36] is used to determine the activation energy of the corrosion process:

$$Ln(i_{corr}) = Ln(A) - \frac{E_a}{RT} \quad (5)$$

Where, A is the Arrhenius constant, R is the molar constant of the gases (8.314 Jmol^{-1}K^{-1}), T(K) the temperature of the solution and E_a (Jmol^{-1}) represents the activation energy of the corrosion reaction.

Fig. 15 represents the plots of i_{corr} as a function of temperature (Eq. 5). It is clear that the dependence between the corrosion rate and temperature follows Arrhenius' law. The fitted E_a value is determined from the slope of the Arrhenius plot, and is found to be 11.5 kJmol^{-1} with R^2=0.98 and A=2.1×10^3 Acm^{-2}. This value is in agreement with the value reported by Benmoussa and al. [13] (13.91 kJmol^{-1}) for steel corrosion in neutral soil (pH 6.7). However, this value is low compared to the value of the activation energy of steel corrosion in simulated

soil solutions obtained by Ikpi and al. [20] 47.01 kJ.mol^{-1} and 42.96 kJmol^{-1} and those in acidic soils which can reach a value of 60 kJ.mol^{-1} [37, 38] and in presence of inhibitors 41.7 kJ mol^{-1} [39].

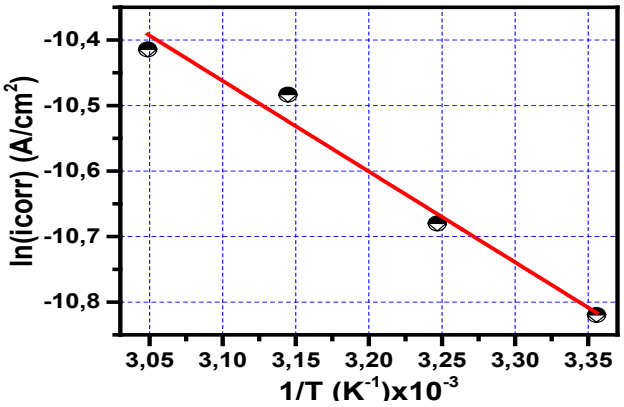

Fig. 15. Arrhenius plot obtained for thesteel corrosion after 6 h in NS4 solution of pH 8.3

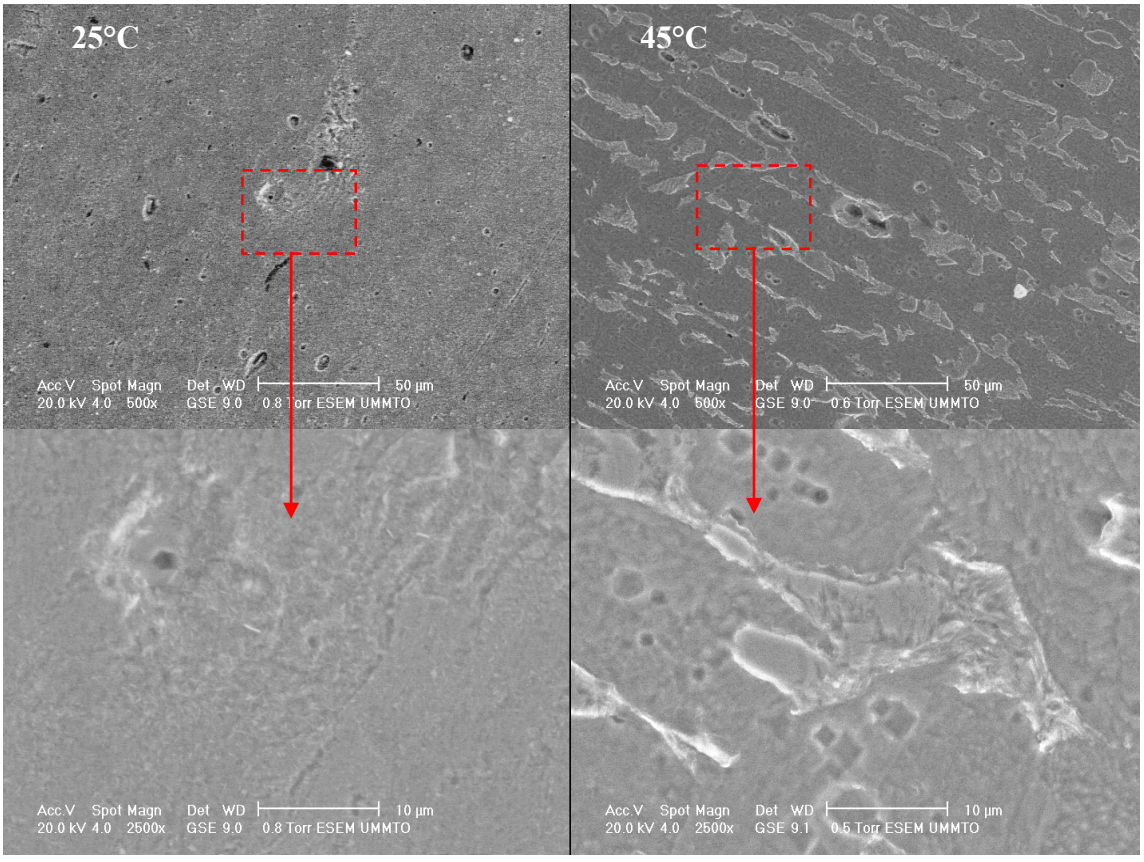

Fig. 16. SEM micrographs of the corroded surfaces of API X52 steel after 6 h immersion in NS4 solution, at 25°C and 45°C

3.3.4. Corrosion morphology

The surface morphologies of X52 steel specimens after 6 h immersion in NS4 solution of pH 8.3, were illustrated in Fig. 16 at 25℃ and 45℃. SEM results at 25 and 45℃ show corroded surfaces. It was observed that at 25°C the corrosion of specimens featured pitting corrosion and when the temperature was raised to 45°C the surface was rough indicating an increase in corrosion. Corrosion rates may be high at higher temperature and pitting may combine to form uniform corrosion.

3.4. Influence of aqueous soil extract

A comparative study was conducted in two different solutions (aqueous soil extract and NS4 solution) of pH = 7.5, for 24 hours of immersion at 25 °C.

3.4.1. Evolution of the open circuit potential

Fig. 17 shows the open-circuit potential of X52 pipeline steel during 24 h of exposure to NS4 solution and aqueous soil extract of pH = 7.5.

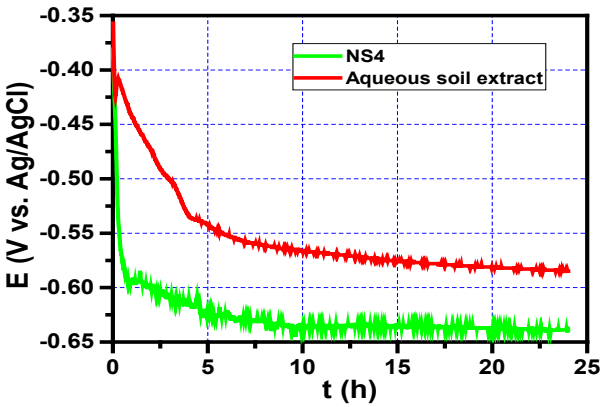

Fig. 17. Evolution of the open-circuit potential versus time for X52 steel at OCP after 24 hours of immersion in NS4 and aqueous soil extract solutions of pH 7.5

It is noticed that the OCP of the sample decreases rapidly in the first few hours of the immersion, which is synonymous of fast dissolution of the steel. After 5 hours of immersion a quasi-stationary state is reached with a lower value of -0.64 V *vs.* Ag/AgCl in NS4 solution compared to the value obtained in the aqueous soil extract (-0.58 V *vs.* AgCl), which means that NS4 solution is more corrosive for steel.

3.4.2. Electrochemical impedance spectroscopy

The EIS measurements of X52 steel conducted at OCP and after 24 hours of immersion in the two different corrosive media, NS4 and aqueous soil extract of pH = 7.5, are shown in Fig. 18. The EIS parameters obtained by fitting according to their best adaptation to the equivalent circuit model shown in Fig. 3d, are listed in Table 9.

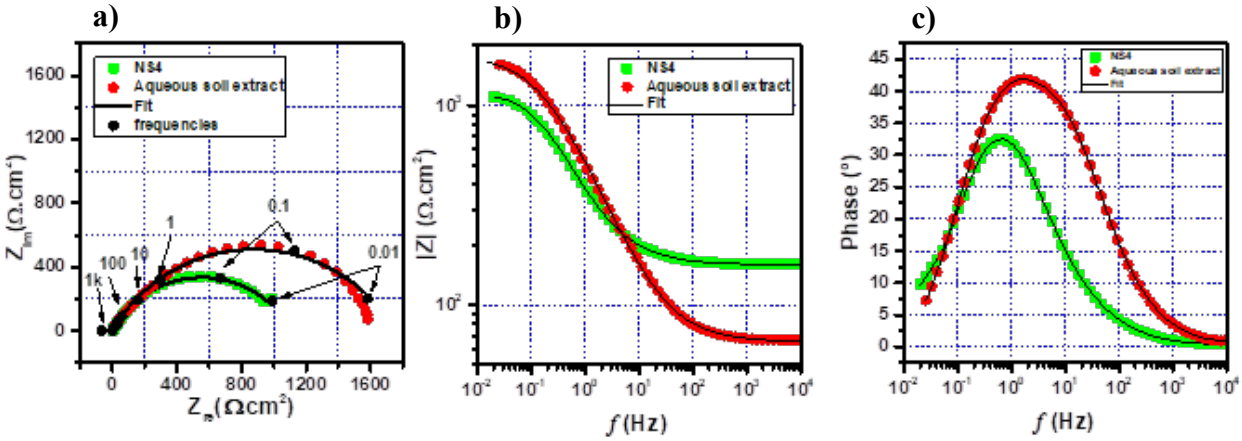

Fig. 18. (a) Nyquist diagrams and (b, c) Bode plots for X52 steel at OCP after 24 hours of immersion in NS4 and aqueous soil extract solutions of pH 7,5

These diagrams show a capacitive behaviour of the interface whose diameter is equivalent to the charge transfer resistance, R_{ct}. It is clear from the figure that the diameter of the semi circle of the aqueous soil extract was much larger than that obtained in NS4 solution. The parameters listed in Table 9 have shown that the value of the polarization resistance, R_{ct}, is higher in the aqueous extract of the soil than in NS4, and at the same time there is a growth in Q. This indicates dissolution of the passive layer and an acceleration of corrosion; this suggests that the corrosion of X52 steel is accelerated in NS4 solution and this is in good agreement with OCP results.

Table 9. Electrical parameters obtained by fit EIS data

Solution	R_s (Ω.cm²)	Q ($Ω^{-1}.cm^{-2}.s^n$)	n	R_{ct} (Ω.cm²)
NS4	126.8	$0.92×10^{-3}$	0.69	1109
Aqueous soil extract	65.0	$0.52×10^{-3}$	0.67	1751

3.4.3. Potentiodynamic polarization curves

Fig. 19 shows the polarization curves obtained for steel X52 in NS4 solution and aqueous soil extract after 24 hours of immersion and the parameters corresponding to the polarization curve are summarized in Table 10.

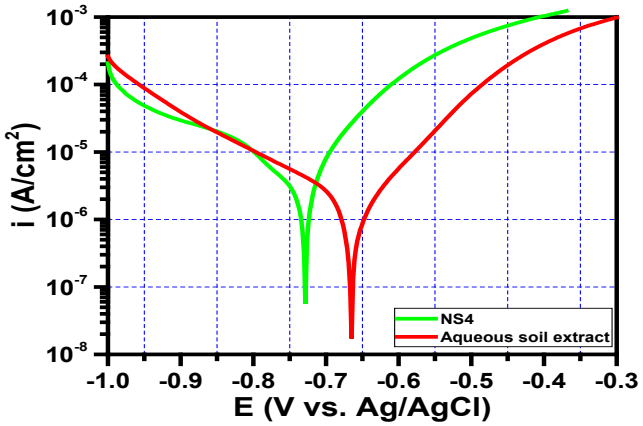

Fig. 19. Potentiodynamic polarization curves for X52 steel at OCP after 24 hours of immersion in NS4 and aqueous soil extract solutions of pH 7.5

It is clear from Fig. 19 that the steel X52 in both solutions is in a state of active dissolution without passivation phenomenon. There is a shift in the corrosion potential of the steel in the NS4 solution towards more electronegative values, accompanied by an increase in the corrosion current density compared to the aqueous soil extract.

In addition, according to the electrochemical parameters summarized in Table 10, the NS4 solution was more aggressive than the aqueous extract of the soil, since the values obtained from i_{corr} and CR were higher, the value of R_p was lower and the value of E_{corr} was more negative than those obtained for X52 steel in the aqueous soil extract, in agreement with the results of Lins and al. [40] The potentiodynamic polarization results are in good agreement with that obtained by EIS and OCP measurements.

Table 10. Values of electrokinetic parameters determined from polarization curves

Solution	E_{corr} (mV *vs.* Ag/AgCl)	i_{corr} (µA/cm²)	$-b_c$ (mV/dec)	b_a (mV/dec)	$R_p \times 10^3$ (Ω.cm²)	$CR \times 10^{-4}$ (mm/y)
NS4	-728	8.1	296	109	4.28	940
Aqueous soil extract	-665	2.0	187	96	13.79	230

3.4.4. Surface analysis by SEM/EDX

SEM micrographs and EDS analysis of the corroded surfaces of API X52 steel after 5 days of free corrosion in NS4 solution and aqueous soil extract are shown in Fig. 20. SEM results indicate that the surfaces of the steel samples were corroded in both test solutions. The total surface area is covered with corrosion products of irregular and porous topography. EDS analysis of the corroded sample in NS4 (image (a)) shows peaks of high intensities relative to

the elements iron, oxygen and calcium with low peak of Mg, indicating the presence of iron oxides with salts in combination. The corroded sample in the aqueous soil extract (image (b)), in addition of the peaks of iron and oxygen, a low peak relative to silicon is obtained, i.e. the corrosion products are mainly iron oxides. Nevertheless, it can be concluded that NS4 solution is more corrosive than aqueous soil extract due to the high concentration of Ca and Mg salts. These results are in good agreement with those of the electrochemical study.

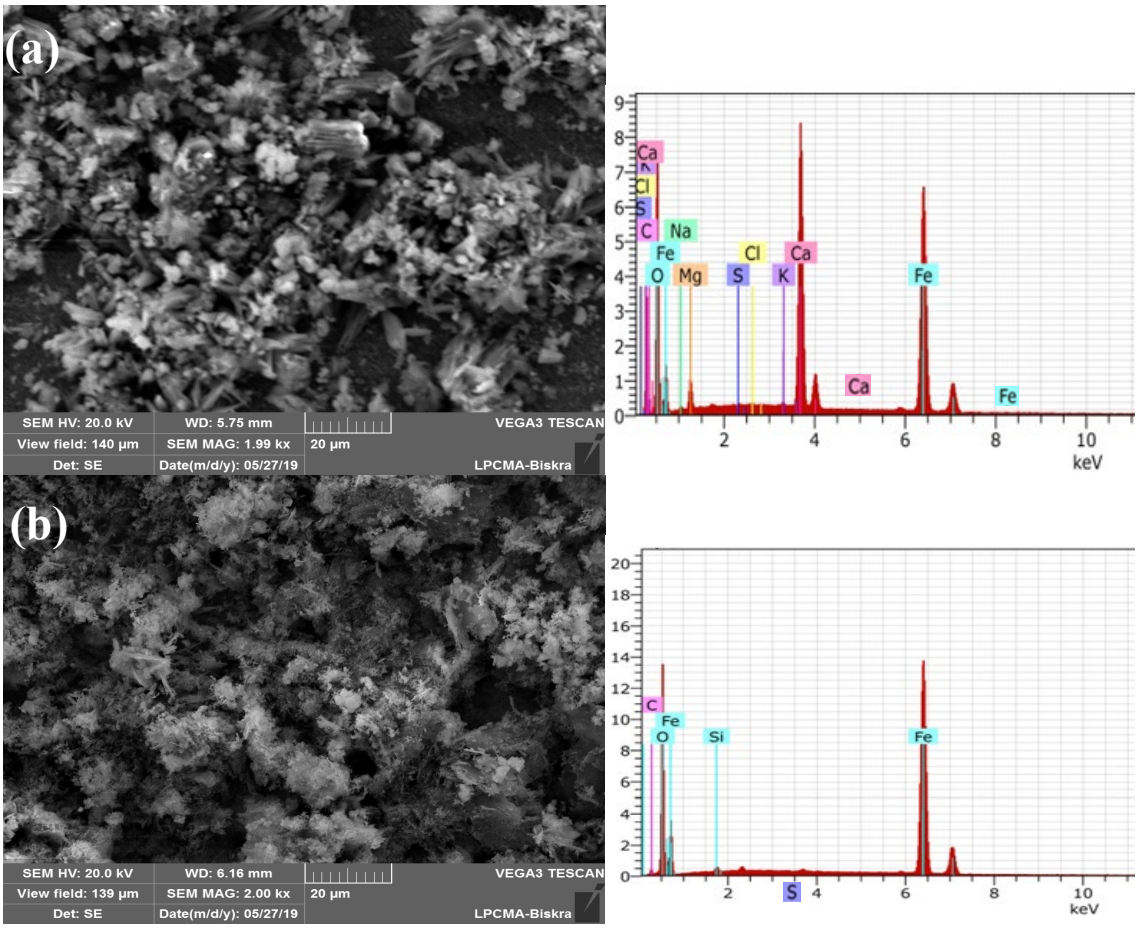

Fig. 20. SEM micrographs and EDS analysis of the corroded surfaces of API X52 steel after 5 days of immersion in (a) NS4 solution and (b) aqueous soil extract

4. CONCLUSION

This work studied the electrochemical corrosion behaviour of API 5L X52 pipeline steel in soil simulation solutions. The results are obtained from multiple measurement methods including free potential, EIS, potentiodynamic polarization and the microscopic morphology. It was demonstrates that soil parameters such as the immersion time, the soil pH and temperature can significantly affect the corrosion of steel buried in the ground.

The results showed that steel corrosion increases, inversely the polarization resistance decreases, when the soil is acid and alkaline and when temperature rises. However, the corrosion rate decreases and inversely the polarization resistance increases, with immersion time up to 3 days then the corrosion increases. This result suggests the formation of a corrosion products film on the surface of the steel which become porous. From the comparative study of NS4 soil solution and aqueous soil extract, it was concluded that the simulated NS4 soil solution is more corrosive than the aqueous soil extract due to its high ions concentration.

Acknowledgements

The authors thank Salem BOUDINAR of the Laboratory of Physics and Chemistry of Materials, University Mouloud Maameri of Tizi-ouzou (Algeria) for the SEM images.

Declarations of interest

The authors declare that they have no known competing financial interests or personal relationships that could have appeared to influence the work reported in this paper.

REFERENCES

[1] J. Brito, and A. T. D. Almeida, Reliab. Eng. Syst. Safe. 94 (2009) 187.
[2] X. Wang, X. Song, Y. Chen, Z. Wang, and L. Zhang, Int. J. Electrochem. Sci. 13 (2018) 6436 .
[3] L. Garverick, Corrosion in the petrochemical industry, Edition ASM international, Mater. Inf. Soc. (1994).
[4] P. S. Rothman, and W. T. Toung, Pipelines, Edition Robert Baboian (2005).
[5] R. Marchal, Oil Gas Sci. Technol. 54 (1999) 649.
[6] P. Altoé, G. Pimenta, C. F. Moulin, S. L. Díaz, and O. R. Mattos, Electrochim. Acta. 41 (1996) 1165 .
[7] S. Sh. Abedi, A. Abdolmaleki, and N. Adibi, Eng. Fail. Anal. 14 (2007) 250 .
[8] P. C. Okafor, X. Liu, and Y. G. Zheng, Corros. Sci. 51 (2009) 761.
[9] N. E. Boukhallat, Prévention et remèdes, corrosion interne des pipes à écoulement multiphasique, MD Media 4 (1998).
[10] P. Shammas, Algeria: review of petroleum, politics and risks, APS Group (1999).
[11] C. Dana, Stop à la corrosion, Market vision, Etats-Unis (2008).
[12] T. M. Liu, Y. H. Wu, S. X. Luo, and C. Sun, Mat. wiss. Werkstofftech 41 (2010) 228 .
[13] A. Benmoussa, M. Hadjel, and M. Traisnel, Mater. Corros, 57 (2006) 771 .
[14] S. R. A. Saupi, M. A. Sulaiman, and M. N. Masri, J. Trop. Resour. Sustain. Sci. 3 (2015) 14.
[15] L. d. Arriba-Rodriguez, J. Villanueva-Balsera, F. Ortega-Fernandez and F. Rodriguez-Perez, Metals 8 (2018) 334 .

[16] B. He, P. J. Han, C. Lu, and X. H. Bai, Mat. wiss. Werkstofftech 46 (2015) 1077 .
[17] B. He, P. J. Han, L. F. Hou, C. H. Lu and X. H. Bai, Mater. Corros 67 (2016) 471 .
[18] B. He, X. H. Bai, L. F. Hou, and D. C. Zhang, Mater. Corros. 2017, 9999, 1 .
[19] B. He and X. Bai, International Conference: Geoenvironment and Geohazard (2018) 346.
[20] M. E. Ikpi, and B. O. Okonkwo, J. Mater. Environ. Sci. 8 (2017) 3809.
[21] L. Wang, Z. Gao, Y. Liu, X. Lu, C. Wang, and W. Hu, Int. J. Electrochem. Sci. 14 (2019) 161 .
[22] P. C. Okonkwo, A. Essam, and A. M. A. Mohamed, Int. J. Electrochem. Sci. 10 (2015) 10246.
[23] M. Corrales-Luna, O. Olivares-Xomet, N. V. Likhanova, R. E. Hernández Ramírez, I. V. Lijanova, P. Arellanes-Lozada, and E. Arce Estrada, Int. J. Electrochem. Sci. 12 (2017) 6729 .
[24] Y. H. Wu, T. M. Liu, S. X. Luo, and C. Sun, Mat.-wiss. U. Werkstofftech. 41 (2010) 142 .
[25] R. Dong, I. Sun, Z. Liu, X. Wang and Q. Liu, J. Iron Steel Res. Int. 15 (2008) 71 .
[26] C. W. Du, X. G. Li, P. Liang, Z. Y. Liu, G. F. Jia and Y. F. Cheng. J. Mater. Eng. Perform. 18 (2009) 216 .
[27] Rihan Omar Rihan, Mater. Res. 16 (2013) 227.
[28] R. N. Parkins, W. K. Blanchard, and B. S. Delanty, Corrosion 50 (1994) 394 .
[29] V. Elias, K. Fishman, B. R. Christopher, and R. R. Berg, U. S. Department of Transportation Federal Highway Administration (2009).
[30] P. Mjwana, M. Mahlobo, O. Babatunde, P. Refait, and P. Olubambi, IOP Conf. Ser.: Mater. Sci. Eng. 430 (2018) 012039.
[31] M. Stern, and A. L. Geary, J. Electrochem. Soc. 104 (1957) 56.
[32] E. S. M. Sherif, R. M. Erasmus and J. D. Comins, Electrochim. Acta 55 (2010) 3657 .
[33] E. S. M. Sherif, Mater. Chem. Phys. 129 (2011) 961 .
[34] E. S. M. Sherif, R. M. Erasmus, and J. D. Comins, Corros. Sci. 50 (2008) 3439 .
[35] M. Es-saheb, E. S. M. Sherif, A. El-Zatahry, M. M. El Rayes, and K. A. Khalil, Int .J. Electrochem. Sci. 7 (2012) 10442.
[36] F. Bentiss, M. Traisnel, and M. Lagrenee, J. Appl. Electrochem. 31 (2001) 41 .
[37] L. Larabi, Y. Harek, O. Benali, and S. Ghalem, Progr. Org. Coat. 54 (2005) 256.
[38] C. Selles, O. Benali, B. Tabti, L. Larabi, and Y. Harek, Mater. J. Environ. Sci. 3 (2012) 206.
[39] S. H. Aljbour, Electrochim. Acta 34 (2016) 407 .
[40] V. F. Cunha Lins, M. L. Magalhães Ferreira, and P. A. Saliba, J. Mater. Resea. Technol. 1 (2012) 161.